

R/C structures strengthened with CFRP Part I: analysis of flexural models

Estruturas de concreto reforçadas com PRFC Parte I: análise dos modelos de flexão



A. L. GAMINO ^a
andre.gamino@gmail.com

T. N. BITTENCOURT ^b
tulio.bittencourt@poli.usp.br

J. L. A. DE OLIVEIRA E SOUSA ^c
jls@fec.unicamp.br

Abstract

This work, presented in two parts, deals with the evaluation of design models for reinforced concrete structures strengthened with Carbon Fiber Reinforced Polymers (CFRP). In this first part, flexural models from ACI 440 and fib-14 guidelines, and recent models available in the literature, are evaluated. These criteria were applied to a total of twenty five beams strengthened in flexure with CFRP composites and tested by the authors: sixteen with rectangular cross section and nine with "T" cross section. Different types of carbon fiber composites (sheets and laminates) were applied, from different manufacturers available in the Brazilian market. Results show a good match among the rupture loads calculated using the ACI-440 guidelines for flexural strengthening and the corresponding values observed in the tests.

Keywords: carbon fiber reinforced polymers, bending strengthening, experimental tests, analytical models.

Resumo

Este trabalho, apresentado em duas partes, trata da avaliação dos modelos de projeto de estruturas de concreto armado reforçadas com Polímeros Reforçados com Fibras de Carbono (PRFC). Nesta primeira parte são avaliados modelos de flexão originados das recomendações ACI-440 e fib-14, assim como outros modelos mais recentes, disponíveis na literatura. Esses critérios foram aplicados a um total de vinte e cinco vigas reforçadas à flexão, ensaiadas pelos autores, das quais dezesseis com seção retangular e nove com seção "T". Foram aplicados diferentes tipos de compósitos de fibras de carbono (tecidos e laminados), de diferentes fabricantes, encontrados no mercado brasileiro. Os resultados obtidos mostram uma boa proximidade entre as cargas de ruptura calculadas de acordo com as recomendações ACI-440 para reforços à flexão e os valores observados nos ensaios.

Palavras-chave: polímeros reforçados com fibras de carbono, reforço à flexão, ensaios experimentais, modelos analíticos.

^a Post-Doctoral Researcher, School of Civil Engineering, Architecture and Urbanism, University of Campinas, andre.gamino@gmail.com, Av. Albert Einstein 951, Campinas-SP, CEP 13083-852.

^b Associate Professor, Polytechnical School, University of São Paulo, tulio.bittencourt@poli.usp.br, Av. Prof. Almeida Prado, 271, São Paulo-SP, CEP 05508-900.

^c Associate Professor, School of Civil Engineering, Architecture and Urbanism, University of Campinas, jls@fec.unicamp.br, Av. Albert Einstein 951, Campinas-SP, CEP 13083-852.

1. Introduction

The use of Fiber Reinforced Polymers (FRP) for strengthening of concrete structures has experienced a significant increase in the last ten years. The easiness of application and the adequate mechanical properties are the key features inducing the quick insertion in the structural strengthening market.

In Brazil specific guidelines for structural strengthening using composite material are not available yet. The current practice is based on international design guidelines or manufacturers' recommendations. The main guidelines currently used for structural strengthening using FRP are: ACI - Committee 440 [1], Bulletin no. 14 of fib [2] and recommendation no. 23 of JSCE [3] - Japan Society of Civil Engineers.

The most popular rupture models for flexural strengthening have been developed based on: shear resistance capacity models, concrete tooth models within cracks and concrete-FRP interface stress models. These models guided the development of experimental work by Gamino [4], whose results, mainly those related to computational modeling of beams strengthened with FRP, are presented in (Gamino; Bittencourt [5]). Different computational programs have been used, such as DIANA®, particularly in the three-dimensional modeling of beams strengthened with FRP to shear (Gamino; Sousa; Bittencourt [6]), or computational development platforms, in which constitutive models and specialized finite elements were implemented for the numerical modeling of cracked concrete, rebars and FRP (Gamino; Bittencourt; Sousa [7]).

2. Analytical Investigation

In this section, some analytical models for the design of flexural strengthening with FRP in RC beams are discussed, based on shear resistance capacity models, concrete tooth models between cracks and models based on the concrete-FRP interface stress.

2.1 Shear Resistance Capacity Models for Flexural Strengthening

2.1.1 Oehlers [8] Model

This model has been developed based on a plated beam loaded in a four or three-point scheme. Assuming that the strengthening ends within the constant moment region, the flexural debonding moment M_{db} can be obtained by:

$$M_{db} = \frac{E_c I_{tr,c} f_{ct}}{0.901 E_f t_f} \quad (1)$$

where:

E_c = modulus of elasticity of concrete;

$I_{tr,c}$ = moment of inertia in Stage II;

f_{ctr} = tensile strength of concrete;

t_f = FRP thickness;

For a plate terminated near the support, it is assumed that debonding occurs when the shear force at the plate end, V_{db} , reaches the shear capacity of the concrete in the RC beam itself, without contribution from the steel stirrups:

$$V_{db} = V_c = (1.4 - (d/2000)) b d (\rho_s f_c)^{1/3} \quad (2)$$

where:

b = width of beam cross section;

ρ_s = ratio of steel tension reinforcement;

f_c = compressive strength of concrete;

In terms of the shear force at the plate end:

$$V_{db,end} = \left(\frac{1.17}{\frac{a}{M_{db}} + \frac{1}{V_{db}}} \right) \quad (3)$$

where:

a = distance from the support to the FRP layer end;

2.1.2 Jansze [9] Model

The critical shear force in RC beam at the FRP end for which debonding occurs is given as follows:

$$V_{db,end} = \tau_{PES} b d \quad (4)$$

where:

τ_{PES} = debonding shear stress;

The debonding shear stresses are given by:

$$\tau_{PES} = 0.18 \sqrt[3]{\frac{d}{B_{mod}}} \left(1 + \sqrt{\frac{200}{d}} \right) \sqrt[3]{100 \rho_s f_c} \quad (5)$$

where:

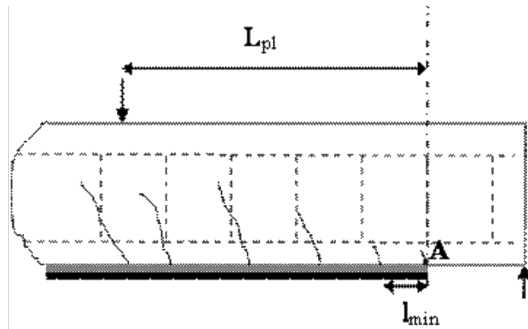
B_{mod} = modified shear span given by:

$$B_{mod} = 4 \sqrt{\frac{(1 - \sqrt{\rho_s})^2}{\rho_s}} d a^3 \quad (6)$$

2.2 Concrete Tooth Models for Flexural Strengthening

Concrete tooth models use the concept of a concrete "tooth" between two adjacent cracks deforming under the action of horizontal shear stresses at the base of the beam. The concept of a concrete "tooth" was first described in Zang; Raoof; Wood [10]. Debonding occurs when these shear stresses add up to tensile stresses at the

Figure 1 – Concrete tooth model



top of the “tooth”, exceeding the tensile strength of the concrete. The stress in the FRP plate at debonding can be determined by defining an effective anchorage length where a uniform shear stress distribution is assumed.

2.2.1 Zang; Raof; Wood [10] Model

The minimum and maximum crack spacing (maximum is assumed

$$l_{min} = \frac{A_e f_{ct}}{0.28 \sqrt{f_c} (\sum O_{rebars} + b_f)} \tag{7}$$

as twice the minimum) can be obtained from: where:

- A_e = area of concrete in tension;
- $\sum O_{rebars}$ = total perimeter of tension reinforced bars;
- b_f = width of FRP layer;

$$\sigma_A = \frac{M_A}{I_A} \left(\frac{l_{cr}}{2} \right) \tag{8}$$

The tensile stress in point “A” (Figure 1) is given by: where:

- l_{cr} = crack spacing, minimum or maximum;
- M_A = bending moment at point “A” (Figure 1);
- I_A = moment of inertia of section corresponding to point “A”;

Assuming that at plate debonding $\sigma_A = f_{ct}$, the shear stress at the interface between the concrete and the FRP plate, based on a minimum stabilized crack spacing, can be determined as follows. In this tooth theory, all teeth in the end anchorage zone are as-

$$\tau_{min} = \frac{f_{ct} l_{min}}{6 h'} \frac{b}{b_f} \tag{9}$$

sumed to fail simultaneously at debonding:

where:

h' = height of concrete cover measured from the base of steel tension reinforcement to the base of concrete beam;

$$\sigma_{min} = 0.154 \frac{L_p h_1 b^2 \sqrt{f_c}}{h' b_f t_f (\sum O_{rebars} + b_f)} \tag{10}$$

Finally the normal stress corresponding to debonding is:

where:

L_p = effective anchorage length;

h_1 = distance from the centroid of the tensile reinforcement to the base of the RC beam;

The effective anchorage length is given by the smaller value be-

$$L_{p2} = l_{min} (21 - 0.25 l_{min}), \quad l_{min} \leq 72 \text{ mm} \tag{11}$$

$$L_{p2} = 3 l_{min}, \quad l_{min} > 72 \text{ mm} \tag{12}$$

tween shear span and the effective anchorage length given by:

2.2.2 Raof; Hassanen [11] Model

Changes in effective anchorage length, described in Equation (11) and Equation (12), were proposed by Raof; Hassanen [11]. The

$$L_{p2} = l_{min} (11.6 - 0.17 l_{min}), \quad l_{min} \leq 56.5 \text{ mm} \tag{13}$$

$$L_{p2} = 2 l_{min}, \quad l_{min} > 56.5 \text{ mm} \tag{14}$$

following lengths which were calibrated with test data of RC beams strengthened with CFRP:

2.3 Interface Stress Based Models to Flexural Strengthening

2.3.1 Varastehpour; Hamelin [12] Model

Varastehpour; Hamelin [12] developed a plate end interface debonding model based on Mohr–Coulomb failure criterion. In their model, the coefficient of cohesion c was calibrated from single lap shear tests and the angle of internal friction ϕ determined from small scale FRP-plated beam tests that failed by

debonding. Average values of 5.4 MPa and 33° were suggested, respectively, for c and φ .

The shear stress required in the Mohr–Coulomb equation is given by:

$$\tau = \frac{1}{2} \sqrt{\beta} (\lambda V_o)^{3/2} \quad (15)$$

where:

V_o = shear force at the FRP layer end;

λ = section rigidity ;

β = factor given by:

$$\beta = \frac{1.26 \cdot 10^5 B}{h^{0.7} t_f E_f} \quad (16)$$

where:

B = shear span;

The following section rigidity is given by:

$$\lambda = \frac{t_f E_f}{I_{tr,c} E_c} (d_f - x) \quad (17)$$

where:

d_f = depth to center of gravity of FRP plate;

The critical shear force in RC beam at the FRP end to cause debonding is given as follows:

$$V_{db,end} = \frac{1.6 \tau_{max}^{2/3}}{\lambda \beta^{1/3}} \quad (18)$$

where:

$$\tau_{max} = \frac{5.4}{1 + C_{R2} \tan 33^\circ} \quad (19)$$

The following cohesion C_{R2} by Roberts [13] is:

$$C_{R2} = t_f \left(\frac{K_n}{4 E_f I_f} \right)^{1/4} \quad (20)$$

where:

I_f = moment of inertia of the FRP plate;

K_n = epoxy (adhesive layer) rigidity given by:

$$K_n = \frac{E_a b_a}{t_a} \quad (21)$$

where:

E_a = modulus of elasticity of the epoxy;

b_a = width of the epoxy layer;

t_a = thickness of the epoxy layer;

2.3.2 Tumialan; Belarbi; Nanni [14] Model

These authors developed a concrete cover debonding model for FRP-plated beams. The model is based on the assumption that a failure criterion for concrete limits the stresses acting on a concrete element at the plate ends.

The shear stresses can be obtained from:

$$\tau = C_{R1} \frac{E_f}{E_c} V_o \quad (22)$$

The cohesion C_{R1} is obtained by (Roberts [13]):

$$C_{R1} = \left(1 + \left(\frac{K_s}{E_f b_f t_f} \right)^{1/2} \frac{M_o}{V_o} \right) \frac{b_t t_f}{I_{tru,c} b_a} (d_f - x) \quad (23)$$

where:

M_o = bending moment at the FRP layer end;

$I_{tru,c}$ = uncracked moment of inertia of the plated section transformed to concrete;

K_s = shear stiffness of the adhesive layer given by:

where:

$$K_s = \frac{G_a b_a}{t_a} \quad (24)$$

G_a = shear modulus of the adhesive layer;

The normal stress σ_y is related to the shear stress as follows:

$$\sigma_y = C_{R2} \tau \quad (25)$$

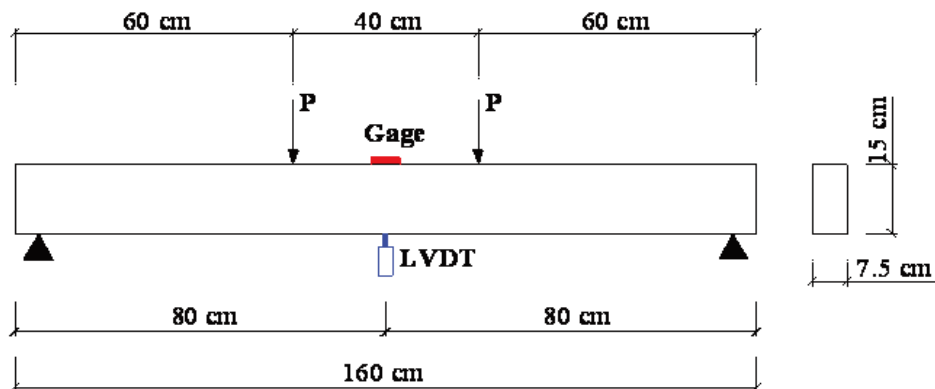
The maximum principal stress is:

$$\sigma_1 = \frac{\sigma_y}{2} + \sqrt{\left(\frac{\sigma_y}{2} \right)^2 + \tau^2} \quad (26)$$

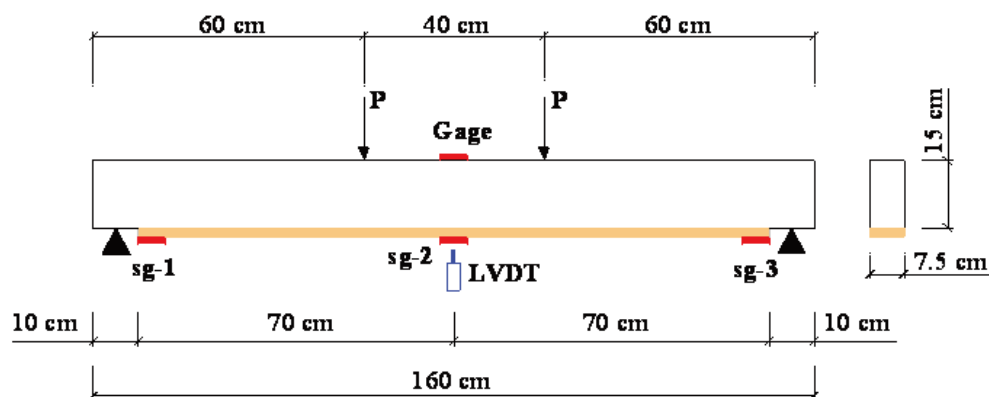
Failure by concrete cover separation is supposed to occur when this maximum principal stress σ_1 reaches the modulus of rupture of the concrete \bar{f} which is taken as $0.689 \sqrt{f_c}$ (MPa) according to Mirza; Hatzinikolas; Macgregor [15].

According to tests by Smith; Teng [16], the answers produced by the model of Tumialan; Belarbi; Nanni [14] produce the same error observed when applying the proposal of Saadatmanesh; Malek [17], whose solution requires more complex procedures.

Figure 2 – Test setup to rectangular beams strengthened in bending with CFRP



a) Control Beams Don't Strengthened with CFRP (Beams RR1 and RR2)



b) Beams Strengthened with CFRP (Beams VR 01 to VR 14)

3. Experimental Procedure

The experimental program included twenty five reinforced concrete beams strengthened with carbon fiber reinforced polymer (CFRP), from which sixteen with rectangular cross section (Figure 2) and nine with "T" cross section (Figure 3).

The mid-span displacements were evaluated using a LVDT; deformations in concrete, reinforcement steel bars and CFRP composites were evaluated using electric strain-gages (KYOWA KFG-5-120-C1-11). Beams RR1 and RR2 were used as reference for rectangular beams and the beams RTF1 and RTF2 were used as reference to "T" beams with CFRP.

The beam VF11 was strengthened with two composites layers and other rectangular beams with one layer. In beams VF12, VF13 and VF14, a non-continuum CFRP fabric was used: in the mid-span anchorage lengths respectively 10 cm, 15 cm and 20 cm were used. All "T" beams were strengthened with two composite layers.

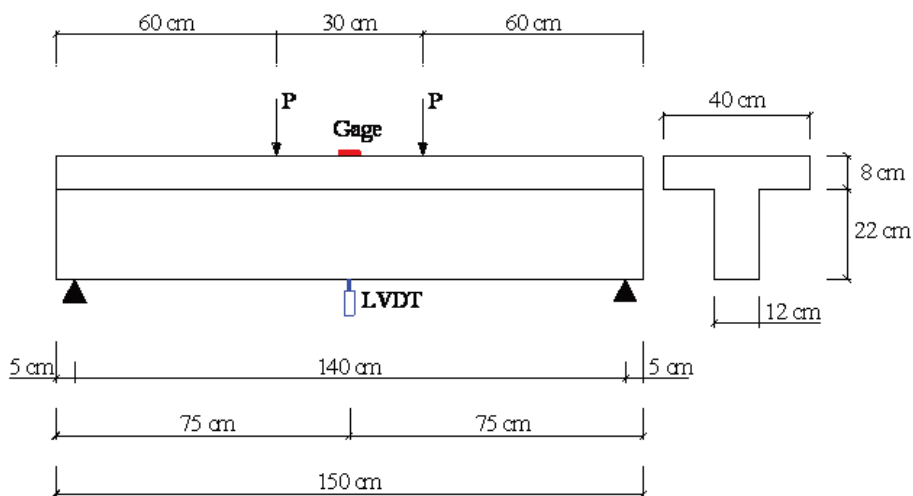
The position of the electric strain-gages in the longitudinal rebars in "T" beams can be observed in Figure 4. The test setup can be visualized in Figure 5. The Lynx data acquisition system ADS 2000 [18] was used in connection with the programs AqDados [19] and AqDAnalysis [20], responsible for control and configuration of the equipment, data reading, writing, visualization and processing.

3.1 Materials

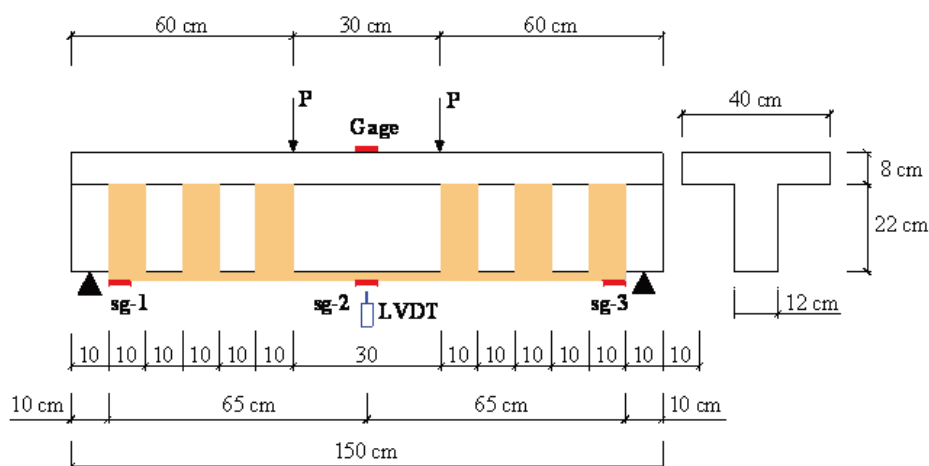
Details of the beams tested in the experimental procedure are illustrate in Table 1, the concrete/reinforcement steel materials properties are presented in Table 2, CFRP and epoxy adhesive properties are indicated, respectively, in Table 3 and 4.

The CFRP characterization tests (see Figure 6) were performed according to ASTM D3039-95 [21], and epoxy adhesive according to ASTM D638-96 [22]. Figure 7 presents the stress-strain curves obtained for used CFRP materials.

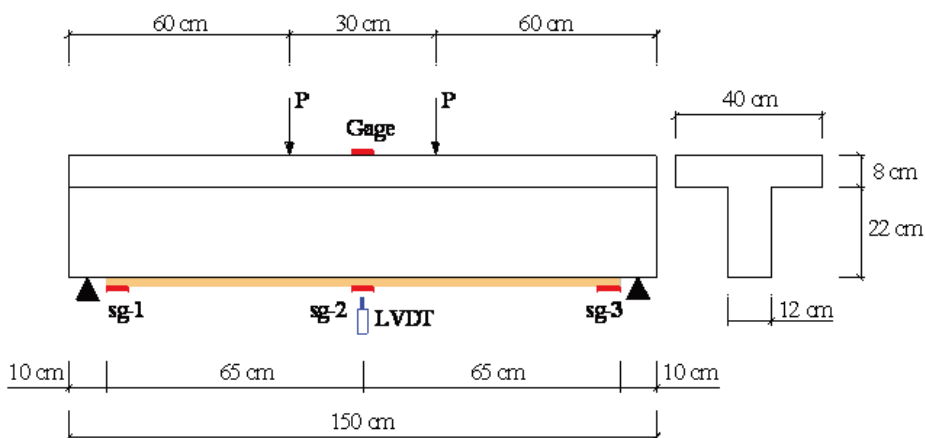
Figure 3 - Test setup to "T" beams strengthened in bending with CFRP



a) Control Beams Don't Strengthened with CFRP (Beams RTF1 and RTF2)

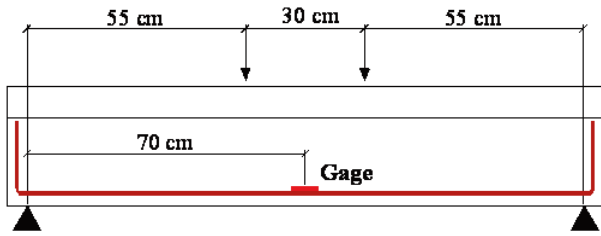


b) Beams Strengthened with CFRP (Beams VTF1 to VTF6)



c) Beam Strengthened with CFRP (Beam VTF7)

Figure 4 – Position of strain-gages in bottom rebars of “T” beams



4. Experimental Results and Discussion

The results obtained in the experimental tests are summarized in Table 5 (for reference beams), Table 6 (for rectangular strengthened beams) and Table 7 (for “T” strengthened beams). The rupture mechanisms found can be observed in Figure 8. The rupture mechanism observed in beams VR 01 to VR 05 was a tensile rupture of CFRP. Evidences of this fact can be observed from the strains in the CFRP measured in the mid-span (Table 6). From the experimental results obtained for strengthened rectangular beams the following observations can be drawn: For VF1 to VF8 beams the bending capacity increased up to 40% (average); for VF9 to VF10 beams the bending capacity increased up to 21% (average); the more brittle behavior was not detected for strengthened beams; from VF1 to VF8 beams the deformation in the CFRP fabric (average) in the mid-span region has been 1.22%; from VF11 beam the bending capacity up to 53% (because two CFRP

fabric layers were used); a similar behavior has been obtained from VF12 to VF14 beams (anchorage length to 10 cm seems to be sufficiently capable of reproducing the behavior of a continuous CFRP fabric according to the design codes).

From the experimental results for “T” beams strengthened in bending, the following observations can be drawn: the least increase in resistance capacity was observed in VTF7 (CFRP sheet without anchorage) and the maximum as an average value from beams VTF3 and VTF4 (82.1%), according to Figure 9-a. In beams VTF1 and VTF2, the strains observed in the bottom reinforcement steel was larger than in the other beams (see Figure 10). All the strengthened beams presented a more fragile behavior in comparison to the reference beams RTF1 and RTF2 (the concrete compressive strains in rupture were smaller in comparison to unstrengthened beams, according to Figure 9-b). The beam VTF7 was the one that showed ductile behavior closest to the reference beams, probably due to least increase in resistance capacity

The general rule is that the gain in load capacity is inversely proportional to the ductile behavior of the structural element, suggesting that a limitation of the load capacity in function of a demanded minimum ductility be established in the design criteria.

5. Comparison of Predictions and Experimentals Results

The comparison among the predictions using the analytical models described in this paper and the described experimental results are shown in Table 8. These results are graphically presented in Figure 11 for rectangular beams and Figure 12 for “T” beams. Results obtained with the expressions from ACI-440 [1] were close to the experimental tests for rectangular beams. In “T” beams strengthened in bending, the obtained results using the fib-14 [2]

Figure 5 – Test scheme



Table 1- Detail of the beams tested in experimental setup

Beam	A_s	Stirrups	CFRP Strength Scheme	CFRP Type	Layers	Width of CFRP (cm)	A_f (mm ²)	Anchorage Length in Mid-Span (cm)
RR1	2 n° 2	n° 2 at 6.0cm	---	---	---	---	---	---
RR2	2 n° 2	n° 2 at 6.0cm	---	---	---	---	---	---
VR 01	2 n° 2	n° 2 at 6.0cm	flexure	CFRP 1	1	7.5	9.75	NO
VR 02	2 n° 2	n° 2 at 6.0cm	flexure	CFRP 1	1	7.5	9.75	NO
VR 03	2 n° 2	n° 2 at 6.0cm	flexure	CFRP 1	1	7.5	9.75	NO
VR 04	2 n° 2	n° 2 at 6.0cm	flexure	CFRP 1	1	7.5	9.75	NO
VR 05	2 n° 2	n° 2 at 6.0cm	flexure	CFRP 1	1	7.5	9.75	NO
VR 06	2 n° 2	n° 2 at 6.0cm	flexure	CFRP 1	1	7.5	9.75	NO
VR 07	2 n° 2	n° 2 at 6.0cm	flexure	CFRP 1	1	7.5	9.75	NO
VR 08	2 n° 2	n° 2 at 6.0cm	flexure	CFRP 1	1	7.5	9.75	NO
VR 09	2 n° 2	n° 2 at 6.0cm	flexure	CFRP 4	1	7.5	8.25	NO
VR 10	2 n° 2	n° 2 at 6.0cm	flexure	CFRP 4	1	7.5	8.25	NO
VR 11	2 n° 2	n° 2 at 6.0cm	flexure	CFRP 4	2	7.5	16.5	NO
VR 12	2 n° 2	n° 2 at 6.0cm	flexure	CFRP 4	1	7.5	8.25	10
VR 13	2 n° 2	n° 2 at 6.0cm	flexure	CFRP 4	1	7.5	8.25	15
VR 14	2 n° 2	n° 2 at 6.0cm	flexure	CFRP 4	1	7.5	8.25	20
RTF1	2 n° 3	n° 1 at 8.0cm	---	---	---	---	---	---
RTF2	2 n° 3	n° 1 at 8.0cm	---	---	---	---	---	---
VTF1	2 n° 3	n° 1 at 8.0cm	flexure	CFRP 2	2	11.5	25	NO
VTF2	2 n° 3	n° 1 at 8.0cm	flexure	CFRP 2	2	11.5	25	NO
VTF3	2 n° 3	n° 1 at 8.0cm	flexure	CFRP 3	2	12	31	NO
VTF4	2 n° 3	n° 1 at 8.0cm	flexure	CFRP 3	2	12	31	NO
VTF5	2 n° 3	n° 1 at 8.0cm	flexure	CFRP 4	2	9	20	NO
VTF6	2 n° 3	n° 1 at 8.0cm	flexure	CFRP 4	2	9	20	NO
VTF7	2 n° 3	n° 1 at 8.0cm	flexure	CFRP 5	1	5	70	NO

CFRP1 and CFRP5 has been used with Sikadur 30 adhesive, CFRP2 with Triepox adhesive, CFRP3 with MBrace Saturant adhesive and CFRP4 with Nitobond CF 55 adhesive.

Table 2 – Concrete and rebars mechanical properties used in tested beams

Rebars					
Bar Size	Diameter (mm)	Area (mm ²)	f_y (MPa)	f_u (MPa)	E_s (GPa)
n° 6	20	314	555	734	198
n° 3	10	78.5	525	756	199
n° 2	6.3	31.2	640	800	180
n° 1	5.0	19.6	517	764	188

Concrete		
Beam	f_c (MPa)	f_t (MPa)
All Rectangular	45	3.6
RTF1	59	4.2
RTF2	57	4.7
VTF1	62	5.0
VTF2	60	5.0
VTF3	60	5.2
VTF4	61	5.6
VTF5	57	5.6
VTF6	59	5.7
VTF7	60	5.8

Table 3 – CFRP mechanical properties

Type	Thickness (mm)	E_f (GPa)	f_{fu} (MPa)	e_{fu} (‰)
CFRP1 ⁱ	0.13	230	3500	15.00
CFRP2 ⁱⁱ	0.11	221	2728	12.44
CFRP3 ⁱⁱⁱ	0.165	218	2730	12.40
CFRP4 ^{iv}	0.11	235	3550	15.00
CFRP5 ^v	1.4	310	1250	4.0

ⁱSika Wrap Hex, ⁱⁱTEI 300, ⁱⁱⁱMBrace, ^{iv}Fosfiber C and ^vSika Carbodur H514.

expressions were closer to the experimental results. For all beams the ultimate loads obtained from ACI-440 [1] expressions were smaller in comparison to those from fib-14 [2] expressions.

The other analytical models described herein did not reproduce satisfactorily the behavior observed in the experiments. Some of them presented limitations that made impossible the analysis in this work, such as Oehlers [8] expressions, which are valid only when the bending moment and the shear forces are high near the region where the FRP layer ends (in the performed tests, the bending moment was very small in the region around the end of the FRP layer). The same occurs with Jansze

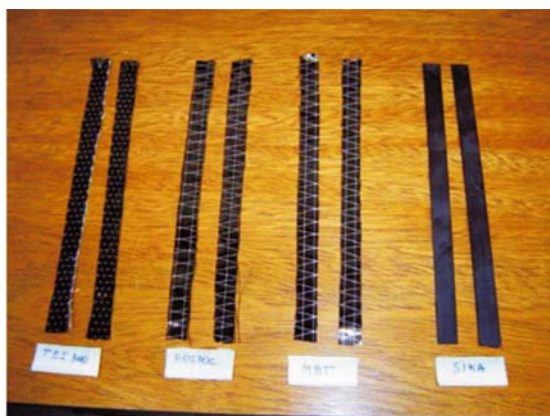
Table 4 – Epoxy adhesive mechanical properties

Type	f_{pu} (MPa)
Triepox	58.9
MBrace Saturant	55.8
Nitobond CF 55	62.2
Sikadur 30	28.4

[9] expressions (such expressions are not valid for sections close to the supports). The results obtained with Zhang; Raouf; Wood [10] model were close to the experimental ones, in opposition to the changes in effective anchorage length proposed by Raouf; Hassanen [11], which produced a result below the experimentally observed. For Tumialan; Belarbi; Nanni [14] model applied to the rectangular beams, the value

obtained for σ_1 was 5.6 MPa, larger than the computed concrete rupture modulus (4.4 MPa), thus suggesting a rupture in the concrete cover together with the debonding of the strengthening layer, as observed experimentally for beams VR 06, VR 07 and VR 08.

Figure 6 – Characterization tests procedure of CFRP



CFRP specimens



Break of CFRP in tensile tests

Such models were not applied to the “T” beams due to difficulties induced by the anchorage mechanism in predicting debonding of the strengthening with the presented analytical models.

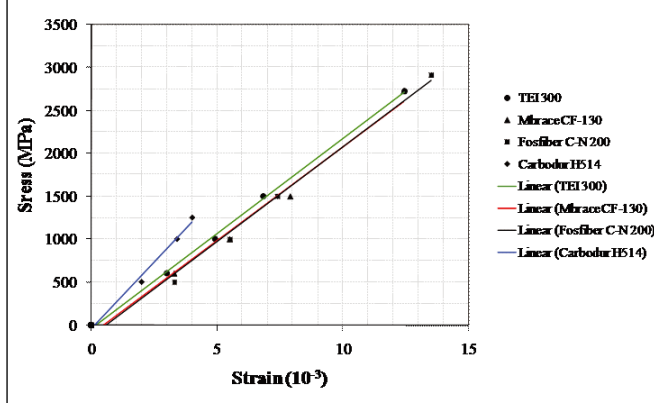
From obtained results to debonding models the values obtained using Zhang; Raof; Wood [10] its closer to experimental results; using Tumialan; Belarbi; Nanni [14] model the obtained value for σ_1 was 5.6 MPa; this value shows most greater to modulus of rupture of the concrete value (4.4 MPa); this suggests that there will be rupture to debonding CFRP layer in agreement to experimental observations to the beams VR 06, VR 07 and VR 08.

6. Conclusions

Based on the results of this experimental investigation, the following conclusions are drawn:

- In the rectangular beams strengthened with FRP the bending capacity increased up to 21% with one CFRP layer

Figure 7 – Strain-stress curves obtained for CFRP materials



and 53% with two CFRP layers. A similar behavior was observed in VF12 to VF14 beams (10 cm anchorage length seemed to be sufficient to reproduce the behavior of a continuous CFRP fabric according to the design codes);

- In the “T” beams a small increment in the bending capacity was achieved with the CFRP5 bonded externally. The absence of an anchorage mechanism induced a premature rupture. Using the material CFRP2, the strains in the tensile reinforcement bars were

larger than the observed in the other strengthened beams. All the “T” beams strengthened with CFRP presented a more brittle behavior than the reference beams.

- Increases in load capacity are inversely proportional to the ductility of the structural element, suggesting that a limitation of the load capacity gain be established in the design criteria as a function of a minimum required ductility for the beams.

Table 5 – Experimental values found to the reference beams

Beam	P _{ref} (kN)	ε _{concrete} (%)	Rupture Mode
RR1	21.3	1.67	flexure
RR2	20.7	2.15	flexure
Average	21.0	1.91	---
RTF1	120	2.20	flexure
RTF2	116	1.98	flexure
Average	118	2.09	---

- The predictions from ACI-440 [1] design code were closer to experimental responses for rectangular beams. In “T” beams strengthened in bending the obtained results using fib-14 [2] expressions were closer to experimental results. For all beams the ultimate loads obtained by ACI-440 [1] expressions were smaller in comparison to the corresponding fib-14 [2] values;
- Zhang; Raouf; Wood [10] and Tumialan; Belarbi; Nanni [14]

models, corresponding, respectively, to the concrete tooth and the concrete-FRP interface stress models, produced good results when applied to FRP strengthened rectangular beams.

7. Acknowledgments

The authors wish to express their gratitude and appreciation to

Table 6 – Experimental values found to the rectangular beams strengthened with CFRP

Beam	P_{max} (kN)	Mid-Span		Anchorage Zone		Δ (%)	Rupture Mode
		$\epsilon_{concrete}$ (‰)	ϵ_f (sg-2) (‰)	ϵ_f (sg-1) (‰)	ϵ_f (sg-3) (‰)		
VR 01	30.77	3.93	13.28	0.89	1.38	47	Break of CFRP
VR 02	28.96	3.12	---	1.65	1.50	38	Break of CFRP
VR 03	30.30	2.26	11.78	0.45	0.78	44	Break of CFRP
VR 04	29.15	2.95	12.56	2.21	1.83	39	Break of CFRP
VR 05	30.39	2.72	11.37	1.90	---	45	Break of CFRP
VR 06	28.77	3.11	---	1.65	1.97	37	Debonding
VR 07	30.55	3.51	---	1.92	1.83	46	Debonding
VR 08	26.35	2.28	---	---	1.12	25	Debonding
Average	29.40	2.98	12.24	1.46	1.45	40	---
VR 9	25.45	1.70	5.33	3.96	3.98	21	Break of CFRP
VR 10	25.35	2.61	6.39	2.88	4.45	21	Break of CFRP
Average	25.40	2.15	5.86	3.42	4.21	21	---
VR 11	32.07	1.33	6.55	---	---	53	Break of CFRP
VR 12	27.40	1.65	4.34	---	---	31	Break of CFRP
VR 13	26.50	2.02	4.42	---	---	26	Break of CFRP
VR 14	28.50	1.46	3.86	---	---	36	Break of CFRP

Table 7 – Experimental values found to the “T” beams strengthened with CFRP

Beam	P_{max} (kN)	Mid-Span			Anchorage Zone		Δ (%)	Rupture Mode
		ϵ_s (‰)	$\epsilon_{concrete}$ (‰)	ϵ_f (sg-2) (‰)	ϵ_f (sg-1) (‰)	ϵ_f (sg-3) (‰)		
VTF1	191	24.3	1.29	6.6	4.9	5.0	61.8	Debonding
VTF2	181	17.2	0.85	5.9	3.1	5.1	53.4	Debonding
Average	186	20.7	1.07	6.2	4.0	5.0	57.6	---
VTF3	210	17.2	1.10	10.1	5.5	6.2	77.9	Debonding
VTF4	220	18.0	1.20	9.9	3.5	6.8	86.4	Debonding
Average	215	17.6	1.15	10.0	4.5	6.5	82.1	---
VTF5	198	10.0	0.99	10.1	4.5	---	67.8	Break of PRFC
VTF6	182	10.5	1.07	10.9	---	4.5	54.2	Debonding
Average	190	10.2	1.03	10.5	4.5	4.5	61.0	---
VTF7	145	9.7	1.66	3.5	1.88	1.98	22.9	Debonding

Figure 8 – Rupture mechanisms found in tested beams



Break of CFRP – VR 01



Debonding of PRFC – VR 07



Break of CFRP – VR 09



Break of CFRP – VR 10

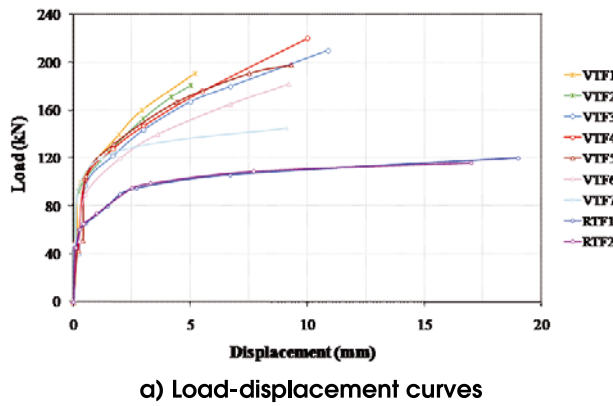


Debonding of CFRP – VTF2

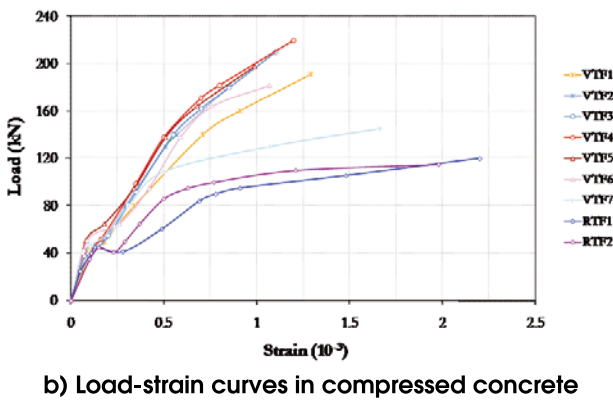


Break of CFRP – VTF5

Figure 9 – Behavior of load capacity and ductility aspect to the “T” beams strengthened with CFRP

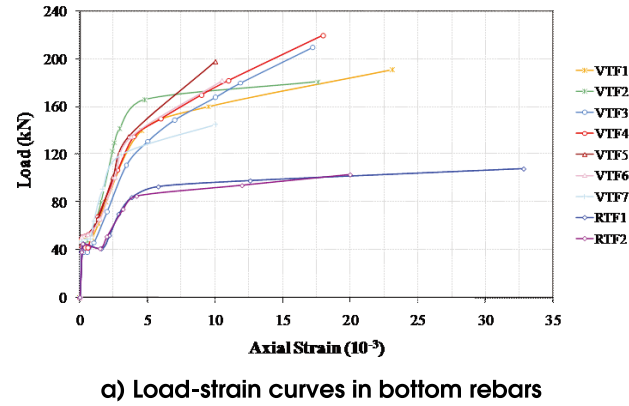


a) Load-displacement curves

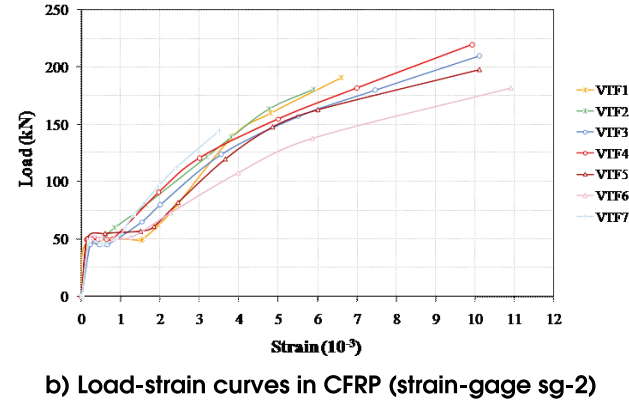


b) Load-strain curves in compressed concrete

Figure 10 – Behavior of strain evolution in rebars and CFRP



a) Load-strain curves in bottom rebars



b) Load-strain curves in CFRP (strain-gage sg-2)

Table 8 – Comparison between analytical and experimental results

Beam	P_{max} (kN)			σ_{min} (MPa)		
	Tests	ACI-440	fib-14	Tests	Zhang; Raouf; Wood (10)	Raouf; Hassanen (11)
VR 01 to VR 08	29.4	26.5	32	2820	2860	590
VR 09/VR 10 and VR 12 to VR 14	26.6	26.9	31.6	---	---	---
VR 11	32.1	31.6	41.8	---	---	---
VTF1/VTF2	186	162	170	---	---	---
VTF3/VTF4	215	190	198	---	---	---
VTF5/VTF6	190	144	154	---	---	---
VTF7	145	159	166	---	---	---

FAPESP – Research Support Foundation of São Paulo State (Processes 06/05843-2, 04/03049-1 and 03/01608-0) and to CNPq – Scientific and Technological Development National Board (Processes 307051/2006-4 and 303735/2008-2) for financing this research work.

8. References

- [01] AMERICAN CONCRETE INSTITUTE. State of the art report on fiber reinforced plastic reinforcement for concrete structures - ACI 440R-02, 2002.
- [02] FEDERATION INTERNATIONALE DU BETON – “BULLETIN 14: Externally bonded FRP reinforcement for RC structures”. Lausanne, October, 2001.
- [03] JAPAN SOCIETY OF CIVIL ENGINEERS. Recommendations for upgrading of concrete structures with use of continuous fiber sheets, JSCE, Concrete Engineering Series, No. 23, 325p., October, 1997.
- [04] GAMINO, A.L., Modelagem física e computacional de estruturas de concreto reforçadas com CFRP. Tese de Doutorado, Escola Politécnica da Universidade de São Paulo, 259p., 2007.
- [05] GAMINO, A.L., BITTENCOURT, T.N., Reinforced Concrete Beams Strengthened with CFRP: Experimental, Analytical and Numerical Approaches. In: 8th International Symposium on Fiber Reinforced Polymer Reinforcement for Concrete Structures - FRPRCS-8, Patras, pp.130-131, CD (10 pages), 2007.
- [06] GAMINO, A.L., SOUSA, J.L.A.O., BITTENCOURT, T.N., Application of Carbon Fiber Reinforced Polymer in Strengthening to Shear R/C T Beams. In: 9th International Symposium on Fiber Reinforced Polymer Reinforcement for Concrete Structures - FRPRCS-9, Sydney, CD (4 pages), 2009.
- [07] GAMINO, A.L., BITTENCOURT, T.N., SOUSA, J.L.A.O., Finite element computational modeling of externally bonded CFRP composites flexural behavior in RC beams. Computers & Concrete, An International Journal, V. 6, No. 3, pp. 187-202, 2009.
- [08] OEHLERS, D.J., Reinforced concrete beams with plates glued to their soffits. Journal of Structural Engineering, ASCE, V. 118, No. 8, pp. 2023-2038, 1992.
- [09] JANSZE, W., Strengthening of RC members in bending by externally bonded steel plates. PhD Thesis, Delft University of Technology, 1997.
- [10] ZHANG, S., RAOOF, M., WOOD, L.A., Prediction of peeling failure of reinforced concrete beams with externally bonded steel plates. Structures and Buildings, V. 110, pp. 257-268, 1995.
- [11] RAOOF, M., HASSANEN, M.A.H., Peeling failure of reinforced concrete beams with fibre reinforced plastic or steel plates glued to their soffits. Structures and Buildings, V. 140, pp. 291-305, 2000.
- [12] VARASTEHPOUR, H., HAMELIN, P. Strengthening of concrete beams using fiber-reinforced plastics. Materials and Structures, V. 30, pp. 160–166, 1997.
- [13] ROBERTS, T.M., Approximate analysis of shear and normal stress concentrations in the adhesive layer of plated RC beams. Structural Engineer, V. 67, No. 12, pp. 229-233, 1989.
- [14] TUMIALAN, G., BELARBI, A., NANNI, A., Reinforced concrete beams strengthened with CFRP composites: failure due to concrete cover delamination. Report CIES-99/01, University of Missouri-Rolla, 1999.
- [15] MIRZA, S., HATZINIKOLAS, M., MACGREGOR, J., Statistical descriptions of the strength of concrete. Journal of Structural Engineering, ASCE, V. 105, pp. 1021-1037, 1979.
- [16] SMITH, S.T., TENG, J.G., FRP-Strengthened RC beams II: assessment of debonding strength models. Engineering Structures, V. 24, No. 4, pp. 397-417, 2002.

Figure 11 – Comparison between analytical and experimental results obtained to rectangular beams

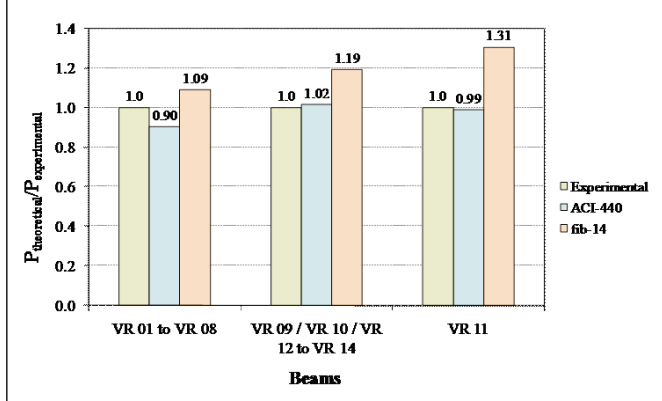
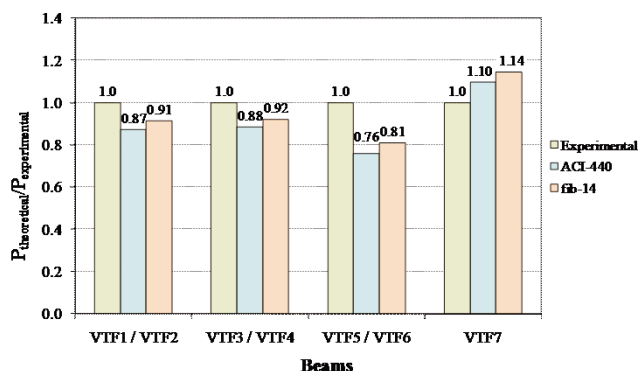


Figure 12 – Comparison between analytical and experimental results obtained to “T” beams strengthened in bending



- [17] SAADATMANESH, H., MALEK, A.M., Design guidelines for flexural strengthening of RC beams with FRP plates. *Journal of Composites for Construction*, ASCE, V. 2, No. 4, pp. 158-164, 1998.
- [18] LYNX TECNOLOGIA ELETRÔNICA LTDA. ADS 2000. Manual de usuário. São Paulo. LYNX, 2003.
- [19] LYNX TECNOLOGIA ELETRÔNICA LTDA. AqDados 7.0 - Programa de aquisição de dados. Manual de usuário. São Paulo. LYNX, 2003.
- [20] LYNX TECNOLOGIA ELETRÔNICA LTDA. AqDAnalysis 7.0 - Programa de tratamento de sinais. Manual de usuário. São Paulo. LYNX, 2005.
- [21] AMERICAN SOCIETY FOR TESTING AND MATERIALS. Standard test method for tensile properties of polymer matrix composite materials. ASTM D3039, 1995.
- [22] AMERICAN SOCIETY FOR TESTING AND MATERIALS, Standard test method for tensile properties of plastics. ASTM D638, 1996.